World Academy of Science, Engineering and Technology
International Journal of Mechanical and Mechatronics Engineering
Vol:2, No:5, 2008

Effect of Fuel Spray Angle on Soot Formation in Turbulent Spray Flames

K. Bashirnezhad, M. Moghiman, M. Javadi Amoli, F. Tofighi, and S. Zabetnia

***Abstract*—**Results are presented from a combined experimental and modeling study undertaken to understand the effect of fuel spray angle on soot production in turbulent liquid spray flames. The experimental work was conducted in a cylindrical laboratory furnace at fuel spray cone angle of 30º, 45º and 60º. Soot concentrations inside the combustor are measured by filter paper technique. The soot concentration is modeled by using the soot particle number density and the mass density based acetylene concentrations. Soot oxidation occurred by both hydroxide radicals and oxygen molecules. The comparison of calculated results against experimental measurements shows good agreement. Both the numerical and experimental results show that the peak value of soot and its location in the furnace depend on fuel spray cone angle. An increase in spray angle enhances the evaporating rate and peak temperature near the nozzle. Although peak soot concentration increase with enhance of fuel spray angle but soot emission from the furnace decreases.

***Keywords*—**Soot, spray angle, turbulent flames, liquid fuel.

I. Introduction

ENVIRONMENTAL concerns along with the limited world oil resources have caused a decrease of the oil consumption on a percentage basis. This decrease is particularly significant in some industrial sectors, such as power generation. However, in other sectors, such as transports, liquid fuels are by far the dominant energy source. In fact, spark ignition engines, diesel engines, gas turbine combustors for aircraft propulsion and rocket engines generally burn liquid fuels. Moreover, due to the increased world energy demand, the world oil consumption has been increasing, mainly because of the contribution of the developing countries. Therefore, the investigation of liquid fuels combustion remains an important research topic.

The role of soot formation in combustion processes is important due to the environmental and health impacts of soot on the one hand, and its important role in radiative heat transfer on the other. Soot formation depends upon the fuel type, as demonstrated, for example, by Glassman's [1] measurements of sooting propensity and smoke-point.

K. Bashirnezhad is with Faculty of Engineering, Islamic Azad University–Mashhad Branch, Iran (corresponding author to provide e-mail: bashirnezhad@yahoo.com).

M. Moghiman and M. Javadi Amoli are with Faculty of Engineering, Ferdowsi University of Mashhad, Mashhad, Iran (e-mails: mmoghiman@yahoo.com, m_javadi_co@yahoo.com).

F. Tofighi is with Faragaman Energy Pak Co.- Mashhad, Iran (tofighi.f4@gmail.com).

S. Zabetnia is with Khavar Part Product Co. (www.kppco.net).

However, it also depends upon oxygen availability and residence time, and so, in turn, upon the mixing characteristics within a flame. This has resulted in the development of numerous burner types with a view to promote [2] or to suppress [3] soot formation.

The effect of mixing, as quantified by the mixing rate, on soot formation has been widely investigated, but mostly in laminar flames because they allow stable and well-defined conditions that cannot be achieved in turbulent conditions.

These technological and environmental concerns emphasize the need for innovative methods to design cleaner combustion devices which can ultimately satisfy stricter emission standards for the particulate matters. The effective control of soot emission requires a comprehensive understanding and modeling of the soot formation and oxidation processes mainly based on the reliable measurements within well-defined flames [4].

The process of soot production from hydrocarbon fuels consists of complex chemical and physical steps, including fuel pyrolysis, formation of polycyclic aromatic hydrocarbons, particle inception, coagulation, surface growth and combustion. Kinetic studies of different workers reveal a dominant kinetic pattern of aromatic-ring growth, H-abstraction C_2H_2-addition [5].

The soot formation model employed in this study is based on the assumption that soot inception and surface growth is a first order function of acetylene concentration. The successful modeling of soot yield also depends on soot combustion model. The OH radical and molecular oxygen O_2 are the most important species in soot oxidation [6].

Typically, flames of liquid fuels have greater soot emission than the gaseous fuels, which is a direct result of diffusion character of these types of flames. Therefore, soot process in this type of flames should be considered more precisely. However, soot processes in spray flames are closely related to atomization, penetration, heating up, and evaporation of droplets [7], [8]. The detailed modeling of the chemistry and physics of soot formation and oxidation in turbulent combustion systems is strongly sensitive to atomization parameters.

In this work, the evolution of soot particles formed during liquid fuel combustion is followed in the atmospheric pressure conditions typical of the furnace combustion chamfer. A reduced mechanism is used to predict the total particulate and the soot formation is modeled by two-parameter, the number

density of the particle (N) and the mass density (M). The results are compared with the experimental measurements.

II. Experimental Apparatus

A atmospheric pressure combustion system designed to provide stable continuous combustion of a liquid spray under reproducible conditions. The system provides sufficient access and time for samples to be taken for analysis from the exhaust and selected locations inside the flame. The full-scale combustor is 360 mm in diameter and 1000 mm in length, that ensures that the essential physics of full-scale combustor are simulated. An oil burner atomizes the pressurized fuel oil inside the combustor. A schematic diagram of the experimental set-up is illustrated in Fig. 1.

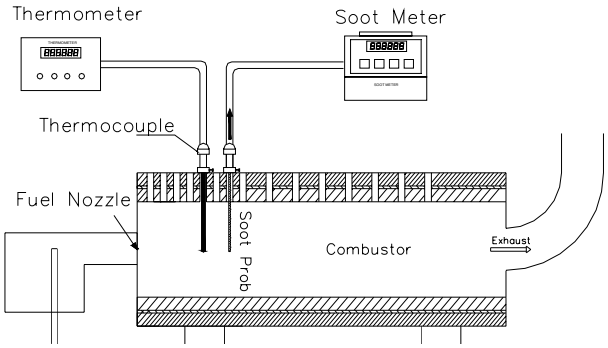

Fig. 1 Schematic of the experimental apparatus

Some rectangular slots are cut into the upper side of the combustor body so that the soot meter and thermocouple probes can be inserted into the center of the cylindrical combustor. Soot concentration is measured using the filter paper technique [9]. The temperature inside the combustor is measured using the ceramic-sheathed type S-thermocouples with a resistance temperature up to 2000 K. The described system measures temperatures within a tolerance of 5 K. Mass flow rate of the fuel is measured by using an analytical scale with the accuracy of 1g. The air into the burner is metered by a rotameter. The temperature of the fuel is maintained at 320 K using an electric heating element. The temperature fluctuation of the inlet air and fuel is kept within the specified margins of 5 K. The repeatability of the data is regularly checked during each experimental session. On average, all of the data can be reproduced to within 10% of the mean value. The combustor flow-gas is continuously monitored during the measurement program to sense any change in the combustor operating conditions. In addition, although every effort is made to eliminate sources of gas leakage in the combustor construction, the combustor pressure is maintained close to atmospheric.

III. The Nozzle

In the combustion chamber, heat is applied to a puddle of oil, causing vapors to be given off from the surface of the fuel. These vapors are then burned after mixing with the proper amount of air. When it is desired to speed up this combustion process, the vaporizing process is accelerated by mechanical means. This is done by breaking the oil up into many extremely small droplets. A very small droplet will, of course, be vaporized in an extremely short period of time when exposed to high temperatures. Also by separating the oil into very small droplets the surface area is increased, exposing more oil surface to contact with air. The simplest method of doing this job with light oils is by the use of nozzles, which separate the fuel into small droplets by their particular design. By this process the surface area is increased by approximately 3800 times. The resultant area of one gallon of fuel is approximately 445 square meters.

Fig. 2 Fuel nozzle

Separation of oil into small droplets requires the application of energy. Fig. 2 shows a fuel nozzle. In the case of nozzles, this energy is supplied in the form of pressure, usually from an appropriately designed motor driven pump. Pressure energy as such will not break up oil it must first be converted into velocity energy. This is done by supplying the fuel under pressure, usually 100 psi on domestic burners, and forcing it through a set of holes or slots. The oil emerges from these slots at very high velocity. Fig. 3 shows a schematic cross section of a pressure-atomizing nozzle. It will be noted that these slots are cut tangentially into a swirl chamber. The high velocity entering streams of oil set up a very high velocity rotation in the swirl chamber. The velocity of rotation increases as the liquid approaches the center of the swirl chamber so that if we place a discharge orifice at the center of this swirl chamber we will have the maximum rotational velocity in that orifice. The velocity of rotation at the center is so high that an air core is created at the center of the vortex. The oil then will extend into the orifice in the form of a rapidly rotating tube of oil, leaving an air core in the center. As this tube of oil is rotating it pushes outward against the walls of the orifice because of the centrifugal force developed. All of the 100-psi pressure supplied at the slots is not converted into velocity energy. Some of it remains as pressure energy and the pressure, which tends to push the liquid

forward through the orifice, will be approximately one half of the applied pressure. This pressure forces the oil to emerge from the orifice in the form of a spinning tube which, because of centrifugal force, immediately expands into a cone shaped sheet as it leaves the orifice. The discharge rate of a nozzle is controlled by the dimensions of the slots and orifice. For best operation a definite relationship between the two must be maintained. The spray angle is governed by the design of the swirl chamber and the orifice.

The principal function of a nozzle then is to break the fuel up into these very small droplets. We use the term "atomize" to describe this process even though it is not strictly correct. The size of these droplets is very important in the performance of a burner. In addition to breaking up the fuel into small droplets, the nozzle is expected to deliver these droplets in a specific pattern. It must be designed to deliver a specified spray angle within specified limits. It must also be designed to distribute these droplets as desired across a cross section of the spray. The common distribution patterns are known as hollow cone and solid cone. In this study are used some solid cone nozzles.

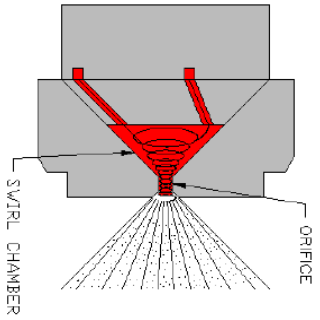

Fig. 3 Schematic of fuel nozzle

IV. Numerical Approach

Computational fluid dynamics is based on the solution of the continuity and Navier–Stokes equations. To take into account the highly irregular nature of turbulence, the components of the velocity vector are usually decomposed in the summation of a mean value and fluctuations; therefore, applying time averaged equations, the continuity, Navier–Stokes and scalar transport equations become:

$$\frac{\partial u}{\partial x}+\frac{1}{r}\frac{\partial}{\partial r}(rv)=\dot{S} \tag{1}$$

$$\frac{1}{r}\left[\frac{\partial}{\partial x}(r\rho uu)+\frac{\partial}{\partial r}(r\rho uv)\right]=-\frac{\partial p}{\partial x}+\mu\nabla^2 u - \frac{1}{r}\frac{\partial}{\partial r}(r\rho\,\overline{u'v'})-\frac{\partial}{\partial x}(\rho\,\overline{u'u'}) \tag{2}$$

$$\frac{1}{r}\left[\frac{\partial}{\partial x}(r\rho uv)+\frac{\partial}{\partial r}(r\rho vv)-\rho w^2\right]=-\frac{\partial p}{\partial r}+\mu(\nabla^2 v+\frac{v}{r^2}) - \frac{1}{r}\frac{\partial}{\partial r}(r\rho\,\overline{v'v'})-\frac{\partial}{\partial x}(\rho\,\overline{u'v'})-\frac{1}{r}\rho\,\overline{w'w'} \tag{3}$$

$$\frac{1}{r}\left[\frac{\partial}{\partial x}(r\rho uw)+\frac{\partial}{\partial r}(r\rho vw)+\rho vw\right]=\mu(\nabla^2 w-\frac{w}{r^2}) - \frac{1}{r}\frac{\partial}{\partial r}(r\rho\,\overline{v'w'})-\frac{\partial}{\partial x}(\rho\,\overline{u'w'})-\frac{1}{r}\rho\,\overline{v'w'} \tag{4}$$

$$\frac{1}{r}\left[\frac{\partial}{\partial x}(r\rho uh)+\frac{\partial}{\partial x}(r\rho vh)\right]=\Gamma_h\nabla^2 h-\frac{1}{r}\frac{\partial}{\partial r}(r\rho\,\overline{v'h'}) - \frac{\partial}{\partial x}(\rho\,\overline{u'h'})+\dot{S}_h \tag{5}$$

Where u and u' are mean and fluctuating axial velocity (m.s^{-1}), v and v' are mean and fluctuating radial velocity (m.s^{-1}) w and w' are mean and fluctuating swirl velocity (m.s^{-1}). The source term is represented by $\dot{S}$ arising from the mass interaction between gas and droplets. P, ρ, μ are pressure (pa), mean density (kg.m^{-3}), and dynamic viscosity (pa.s) respectively. h, Γ_k, $\dot{S}_h$ are enthalpy (j), the turbulent diffusivity and chemical source term respectively. In the view of inability of the k-ε model to cope with anisotropic flows [10], the turbulent stresses are calculated from an algebraic stress model [11]. In addition, a conventional wall-function approach is used in the near-wall region to bridge the viscous sublayer.

Another term that needs to be modeled is the chemical source term $\dot{S}_h$ in Eq. (5). Some of the most widely used modeling approaches are the Eddy dissipation model, the transported probability density function (PDF) method, the presumed PDF method and the laminar flamelet model. In this work the presumed a reduced mechanism is employed, representing a good trade-off between CPU time and accuracy [12].

The mathematical model is based on a typical Eulerian gas phase and a Lagrangian fuel droplet phase formulation. Since a one-way interaction model is used for the gas flow and the droplets trajectory analysis, the air flowfield is firstly evaluated whereas the results are used for evaluation of the droplets trajectories.

The velocity, mass and temperature history of all fuel droplet groups along their trajectories are obtained from the respective conservation equations on a Lagrangian frame [13]. The range of droplet size is considered to be in the range of 10 to 100 μm to be consistent with the experiment, ten droplet group sizes are assumed in this range and calculation is performed for each of the droplet sizes [14].

V. Soot Modeling

The emission of soot from a flame is determined by a competition between soot formation and oxidation that must be considered when a soot modeling study is carrying on. In this study, a recent soot model developed by Moss et al. [15], is used. The model describes the soot formation in terms of the soot particle number density (N) and the soot particle mass density (M) and takes into account the inception (nucleation), coagulation, growth and oxidation processes for

the rates of these two model parameters as:

$$\frac{DN}{Dt}=\left(\frac{dN}{dt}\right)_{Inception}+\left(\frac{dN}{dt}\right)_{Coagulation} \quad (6)$$

$$\frac{DM}{Dt}=\left(\frac{dM}{dt}\right)_{Inception}+\left(\frac{dM}{dt}\right)_{Growth}+\left(\frac{dM}{dt}\right)_{Oxidation} \quad (7)$$

The acetylene inception model is used for the calculation of soot inception rate according to Brookes & Moss, [3], and Lueng et al. [17].

Taking into account that presence of aromatics in kerosene enhances inception, the inception rates are computed by:

$$\left(\frac{dN}{dt}\right)_{Inception}=c_1 N_A\left(\rho\frac{m_{C_2H_2}}{W_{C_2H_2}}\right)e^{-21100/T} \quad (8)$$

$$\left(\frac{dM}{dt}\right)_{Inception}=\frac{M_P}{N_A}\left(\frac{dN}{dt}\right)_{Inception} \quad (9)$$

Where M_p=144 kg.kmol^{-1}, N_A is Avogadro's number and c1=84 s^{-1}. W_{C2H2} and m_{C2H2} are molecule weight and mass fraction of acetylene species. T is temperature (k).

Assuming the particles are mono-dispersed in size and spherical, the coagulation rate and reaction surface are given by:

$$\left(\frac{dN}{dt}\right)_{coagulation}=-\left(\frac{24R}{\rho_{Soot}N_A}\right)^{1/2}\times\left(\frac{6}{\pi\rho_{Soot}}\right)^{1/6}T^{1/2}M^{1/6}N^{11/6} \quad (10)$$

$$\left(\frac{dM}{dt}\right)_{growth}=c_2\left(\rho\frac{m_{C_2H_2}}{W_{C_2H_2}}\right)e^{-21100/T}\times\left((\pi N)^{1/3}\left(\frac{6M}{\rho_{Soot}}\right)^{2/3}\right) \quad (11)$$

where R is the universal gas constant, ρ_{soot}=2000 kg.m^{-3} and c2=10010 kg.m.kmol^{-1}.s^{-1}.

The soot oxidation model takes into account oxidation of soot both by O_2 and OH radicals. In this model, the rate of soot oxidation is given by,

$$\left(\frac{dM}{dt}\right)_{Oxidation}=-c_4\rho\eta\frac{m_{OH}}{W_{OH}}\sqrt{T}(\pi N)^{1/3}\left(\frac{6M}{\rho_{Soot}}\right)^{2/3}-c_3\rho\frac{m_{O_2}}{W_{O_2}}\exp(\frac{-19778}{T})\sqrt{T}(\pi N)^{1/3}\left(\frac{6M}{\rho_{Soot}}\right)^{2/3} \quad (12)$$

where η is set to be 0.13, c3 = 8903.51 kg.m.kmol^{-1}.K$^{-1/2}$, c4=105.81 kg.m.kmol^{-1}.K$^{-1/2}$.s^{-1}, which are obtained by converting the rate of soot mass consumption [3].

The gas conservation equations are solved using a two-dimensional control-volume based computational procedure. The convective terms are discretized by the power law scheme. The flow field pressure linked equations are solved by the SIMPLE algorithm and the set of algebraic equations are solved sequentially with the line-by-line method which is a combustion of Gauss-Seidel method and tridiagonal-matrix algorithm. The convergence criterion is determined by the requirement that the maximum value of the normalized residuals of any equation must be less than 1×10^{-5}. Under-relaxation factor is chosen as 0.3 for all dependent variables.

Because of elliptic nature of the conservation equations, boundary conditions are specified at all boundaries of the domain considered. The air enters the combustor with the temperatures of 298K and with the axial velocity of 3 m.s^{-1}. Mass flow-rate of the liquid fuel, which is injected at 323 K, equals to 0.05 kg.s^{-1} whereas different spray cone angles are investigated. In addition, at the outlet, for all variables, a zero axial gradient is prescribed.

Typical mesh distribution for the combustion chamber is illustrated in Fig. 4. For simulations of combustion chamber fine mesh densities were employed to resolve the flow, turbulence, combustion, and soot processes. Considering the furnace structure as the purpose of illustration for grid independence, three grid meshes were tested: a coarse grid of 100×50 with 5000 nodes, a medium grid of 180×90 with 16200 nodes and a fine grid of 240×120 with 28800 nodes. Small differences existed between the predicted temperature distributions between the medium and fine grids. The coarse grid was seen, however, to grossly over-predict the temperatures at the inlet of the furnace. The maximum difference between the three grids was, however, less than 2%. Comparison with the experimental data for the medium and fine grids showed that both could provide reasonable results. It is therefore concluded that the resolution of the fine grid should be sufficient and predictions hereafter in the following are all based on the fine grid system. The grid spacing in axial and radial directions are changed smoothly to minimize the deterioration of the formal accuracy of the discretization scheme due to variable grid spacing and in such a way that higher concentration of nodes occur near the inlet and the walls.

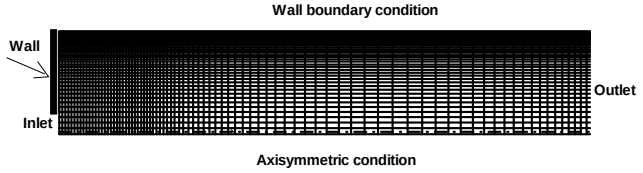

Fig. 4 Mesh distribution for combustion chamber

VI. Result and Disscussions

The temperature domain is the most important parameter on soot production. Fig. 5 shows effect of fuel spray angle on centerline temperature profile. The results show that fuel spray cone angle is the important character has a profound effect on the temperature profile. Comparison of the experimental results of the three-fuel spray cone angles reveals that an increase in fuel spray cone angle increases the combustor centerline temperature levels. This is due to the droplet size is smaller in the wider spray angles. So an increase size of spray cone zone increased mixing rates between the fuel droplets and oxidant.

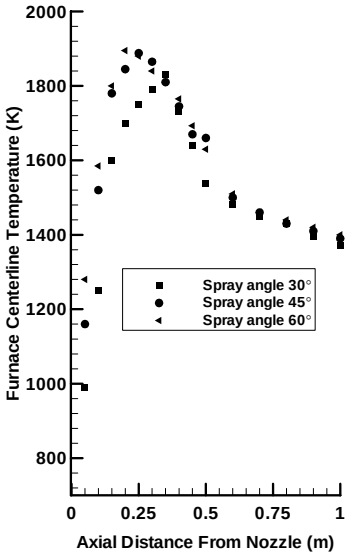

Fig. 5 Measurements of centerline temperature profiles for three fuel spray cone angles

Experimental results for effect of fuel spray angle on soot volume fraction distribution inside the combustor are shown in Fig. 6. It can be seen that the maximum soot volume fraction occurs in the vicinity of the fuel injection point where the fuel concentration and temperature level are high there. This occurs because the process of soot nucleation and surface growth are strongly temperature and fuel concentration dependent. The comparison of the results of the three fuel spray angles reveals that an increase in the fuel spray cone angle increases the soot volume fraction levels near the nozzle. The on-line measurement of the soot volume fraction exiting the furnace shows with increase the fuel spray cone angle decrease soot volume fraction exhaust from the furnace.

Figs. 7 shows measured and predicted centerline temperature profiles for three fuels spray cone angle. It is seen that the agreement between predicted and measurement data is very good. Comparison of three spray cone angle shows that the fuel injected from lower spray angle penetrates longer axial distance into the gas flow. The results showed that the nearly complete dissociation of fuel is dependent of fuel spray cone angle.

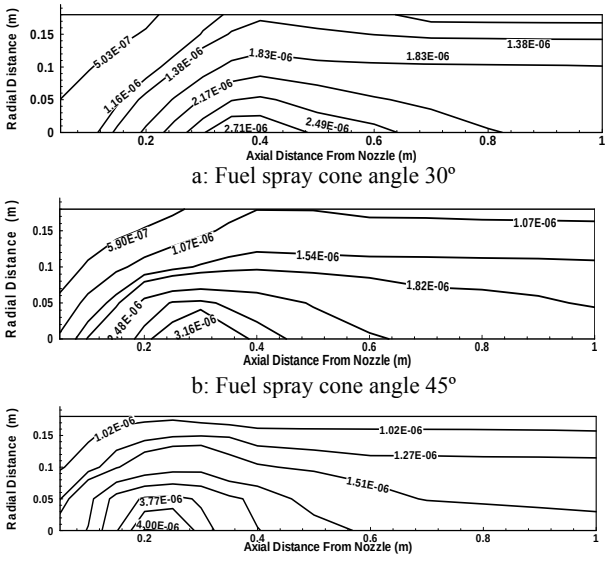

Fig. 6 Measured soot volume fraction distributions inside the combustor for different fuel spray angles

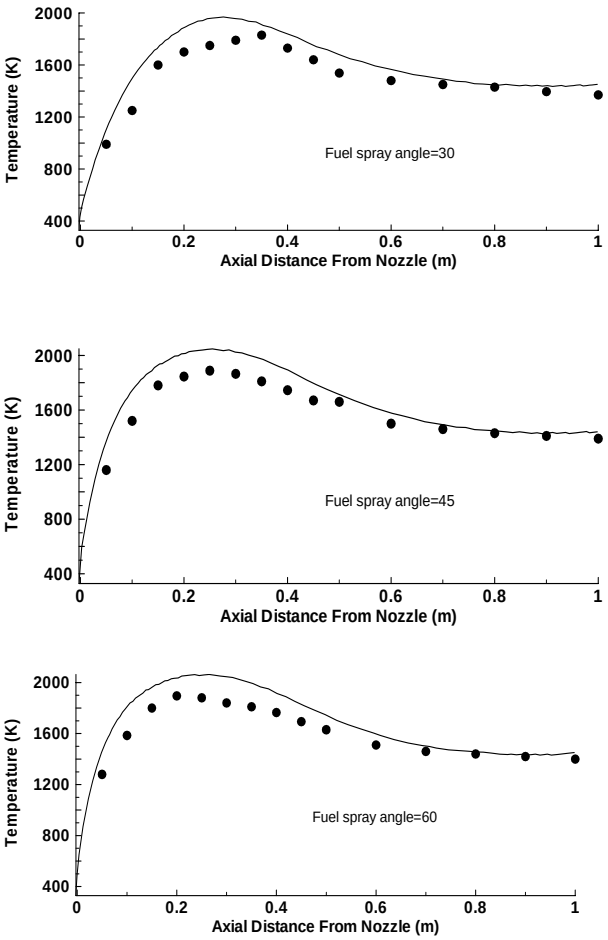

Fig. 7 Comparison between prediction and measurements of centerline temperature

The comparisons between the computed results with experimental data of soot concentration are shown in Fig. 8. The comparison of the results of the three fuel spray angles reveals that an increase in the fuel spray cone angle increases the soot volume fraction levels near the nozzle. The fuel injected from lower spray angle penetrates longer axial distance into the gas flow and produce higher soot volume fraction near the outlet of the combustor. The predictions results have a good agreement with the experimental data.

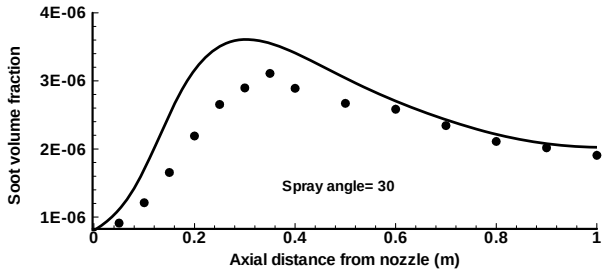

a: Fuel spray cone angle 30º

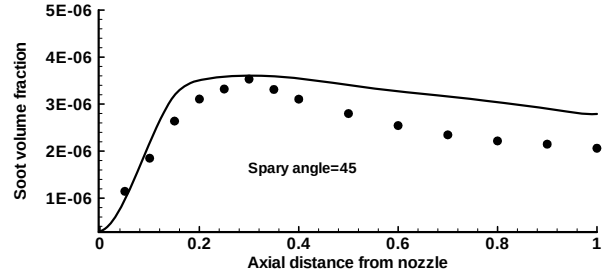

b: Fuel spray cone angle 45º

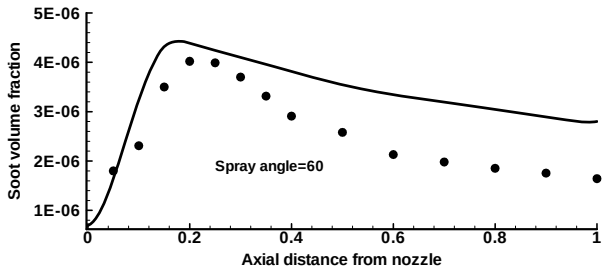

c: Fuel spray cone angle 60 º

Fig. 8 Comparison between the centerline soot volume fractions with the experimental data

VII. Conclusion

The experimental and perdition results showed that the fuel spray cone angle has a significant influence on flame structure and temperature profiles. The maximum temperature of the flame is enhanced with the fuel spray angle increased. The results showed that the nearly complete dissociation of fuel is dependent of fuel spray cone angle. Also spray angle has a strong effect on the soot volume fraction. The on-line measurement of the soot volume fraction exiting the furnace shows with increase the fuel spray cone angle decrease soot volume fraction exhaust from the furnace. The maximum soot volume fraction has occurred in spray cone angle 60° although in this spray cone angle the soot exit from furnace is minimize. The complete furnace simulation shows large soot volume fraction gradients in the axial and radial directions. Both the numerical and experimental results show that the peak value of soot and its location in the furnace depend on fuel spray cone angle.

Acknowledgment

The support of the K.P.P CO. (Khavar Part Product Company) is gratefully acknowledged.

References

[1] I. Glassman, "Sooting laminar diffusion flames, effect of dilution, additives, pressure, and microgravity," Proc Combust Instit, 27:1589 (1998).

[2] J. F. Roesler, S. Martinot, C. S. McEnally, L. D. Pfefferle, J. L. Delfau, and C. Vovelle, "Investigating the role of methane on the growth of aromatic hydrocarbons and soot in fundamental combustion processes," Comb. Flame J., vol. 134, pp. 249-260, 2003.

[3] S. J. Brookes, and J. B. Moss, "Predictions of soot thermal radiation properties in confined turbulent jet diffusion flames," Comb. Flame J., vol. 116, pp. 486-503, 1999.

[4] T. M. Gruenberger, M. Moghiman, P. J. Bowen and N. Syred, "Dynamic of soot formation by turbulent combustion and thermal decomposition of natural gas," Comb. sci. tech. J., vol. 174, pp. 67-86, 2002.

[5] B. Yang, and U. O. Koylu, "Detailed soot field in a turbulent non-premixed ethylene/air flame from laser scattering and extinction experiments," Comb. Flame J., vol. 141, pp. 55-65, 2005.

[6] A. Beltrame, P. Porshnev, W. Merchan-Merchan, A. Saveliev, A. Fridman, L. A. Kennedy, O. Petrova, S. Zhdanok, F. Amouri. O. and Charon, "Soot and NO Formation in Methane–Oxygen Enriched Diffusion Flames," Comb. Flame J., vol. 124, pp. 295-310, 2001.

[7] M. Moghiman, and M. R Maneshkarimi, "On the dependence of spray evaporation and combustion on atomization techniques," Iranian Sci. Tech. J., vol. 25, pp. 241-252, 2001.

[8] M. Sommerfeld, and H. H. Qiu, "Experimental studies of spray evaporation in turbulent flows," Heat Fluid Flow J., vol. 19, pp. 10-22, 1998.

[9] AVL Smoke Measurement, AVL LIST GMBH, Graz (2001).

[10] A. E. German, and T. Mahmud, "Modeling of non-premixed swirl burner flows using a Reynolds-stress turbulence closure," Fuel J., vol. 84, pp. 583-594, 2005.

[11] J. Zhang, S. Nieh, and L. Zhou, "A new version of algebraic stress model for simulating strongly swirling flows," Numerical Heat Transfer J., vol. 22, pp. 49-62, 1992.

[12] P. M. Patterson, A. G. Kyne, M. Pourkashanian, A. Williams, and C. W. Wilson, "Combustion of kerosene in counter flow diffusion flames," Propulsion Power J., vol. 6, pp. 453-460, 2001.

[13] C. K. Westbrook, and F. L. Dryer, "Simplified reaction mechanisms for the oxidation of hydrocarbon fuels in flames," Comb. Sci. Tech. J., vol. 27, pp. 31-45, 1981.

[14] N. Y. Sharma, and S. K. Dom, "Influence of fuel volatility and spray parameters on combustion characteristics and NOx emission in a gas turbine combustor," Applied Thermal Eng. J., vol. 24, pp. 885-903, 2004.

[15] J. B. Moss, C. D. Stewart, and K. J. Young, "Modeling soot formation and oxidation in a high temperature laminar diffusion flame burning under oxygen-enriched conditions," Comb. Flame J., vol. 101, pp. 491-500, 1995.

[16] G. M. Faeth,, "Evaporation and combustion of sprays," Prog. Energy Comb. Sci. J., vol. 9 pp. 1-76, 1983.

[17] K. M Lueng, R. P. Lindstedt, and W. P. Jones, "A simplified reaction mechanism for soot formation in non premixed flames," Comb. Flame J., vol. 87, pp. 289-305, 1991.

[18] Z. Wen, S. Yun, M. J. Thomson, and M. F. Lightstone, "Modeling soot formation in turbulent kerosene/air jet diffusion flames," Comb. Flame J., vol. 135, pp. 323-340, 2003.